Spin Rings in Bistable Planar Semiconductor Microcavities

C. Adrados,[1] A. Amo,[1] T. C. H. Liew,[2] R. Hivet,[1] R. Houdré,[3] E. Giacobino,[1] A. V. Kavokin,[4] and A. Bramati[1]

[1]*Laboratoire Kastler Brossel, Université Pierre et Marie Curie-Paris 6, École Normale Supérieure et CNRS, UPMC Case 74, 4 place Jussieu, 75005 Paris, France*

[2]*Institute of Theoretical Physics, École Polytechnique Fédérale de Lausanne, CH-1015, Lausanne, Switzerland*

[3]*Institut de Physique de la Matière Condensée, Faculté des Sciences de Base, bâtiment de Physique, Station 3, EPFL, CH 1015 Lausanne, Switzerland*

[4]*Physics and Astronomy School, University of Southampton, Highfield, Southampton, SO171BJ, United Kingdom*

(Received 20 July 2010; revised manuscript received 22 September 2010; published 15 November 2010)

A remarkable feature of exciton-polaritons is the strongly spin-dependent polariton-polariton interaction, which has been predicted to result in the formation of spin rings in real space [Shelykh *et al.*, Phys. Rev. Lett. **100**, 116401 (2008)]. Here we experimentally demonstrate the spin bistability of exciton polaritons in an InGaAs-based semiconductor microcavity under resonant optical pumping. We observe the formation of spin rings whose size can be finely controlled in a spatial scale down to the micrometer range, much smaller than the spot size. Demonstration of optically controlled spin patterns in semiconductors opens way to the realization of spin logic devices and spin memories.

DOI: 10.1103/PhysRevLett.105.216403 PACS numbers: 71.36.+c, 42.65.Pc, 72.25.Fe

Spin-dependent particle-particle interactions give rise to a rich variety of effects in nonlinear optics [1,2]. They are of particular interest in semiconductors, due to the high integrability capabilities, microstructuring, and easy electric and optical control in these materials [3]. However, spin-dependent interactions in semiconductors are very weak due to the dominant role of the direct Coulomb interaction. The use of semiconductor microcavities in the strong exciton-light coupling regime allows for observation of spin-dependent nonlinear effects, such as spin-dependent energy shifts and multistability, at very low pumping power [4,5].

Polaritons are the eigenstates in semiconductor microcavities, arising from the strong coupling between quantum well excitons and confined photon modes. They have two possible spin projections on the structure's axis ($s_z = +1$ and -1), and can be excited, and detected, via circularly polarized photons (σ^+ and σ^-, respectively).

The main signature of the strong coupling is the appearance of a normal-mode (Rabi) splitting between polariton modes [6]. This splitting gives rise to a strong asymmetry in the interaction strength between polaritons of the same and opposite spin [7–9]. Polaritons with parallel spins lying at the bottom of the dispersion curve strongly repel each other due to the Coulomb exchange interaction between electrons and between holes (interaction strength α_1). On the other hand, in the antiparallel spin configuration the exchange interaction would result in intermediate states in which the total spin of each exciton is ± 2, thus being uncoupled to the photon modes, and lying at the exciton level located at a quite different energy to that of the considered polaritons. For this reason, this interaction process is strongly inhibited, resulting in a reduced antiparallel spin polariton-polariton interaction strength α_2 ($\alpha_1 \gg |\alpha_2|$) [5,10] which, additionally, should be attractive according to second order perturbation theory [7,8]. This mechanism can be enhanced by biexcitonic effects [7]. In this work, we take advantage of the strongly spin-dependent polariton-polariton interactions, in the regime of spin-bistability [4,11], to control the polariton spin state on a spatial scale much smaller than the size of the optical excitation spot. Following the recent proposal by Shelykh *et al.* [12] we demonstrate the creation of ''spin rings'' within the excitation spot, whose size can be finely tuned by the intensity and degree of circular polarization of the excitation beam. Additionally, we demonstrate nonlinear interactions between polariton populations of opposite spin, a consequence of the nonvanishing value of α_2, whose magnitude and sign we precisely determine for our experimental conditions. Our results are well reproduced by the solution of the spin-dependent Gross-Pitaevskii equation (GPE) for the polariton system [13,14].

Our experiments are performed at 6 K in an InGaAs/GaAs/AlGaAs planar microcavity with a Rabi splitting of 5.1 meV, and a polariton linewidth of 0.1 meV at zero exciton-cavity detuning [15]. The excitation is performed at normal incidence with a polarized beam of controlled ellipticity coming from a cw single-mode Ti:sapphire laser, in a Gaussian spot of 38 μm in diameter. We measure the polarization resolved transmitted light [16].

When the sample is excited with σ^+ polarized light with photon energy 0.124 meV blue-detuned from the lower polariton branch (LPB), we observe a steplike behavior in the transmitted intensity versus the excitation density, with a hysteresis cycle [Fig. 1(a)] giving rise to a bistable region [11], between excitation densities D_1 and D_2. This nonlinear transmission arises from the renormalization of the dispersion curve when the polariton density is

increased via the excitation power. When the system is in the off state (lower bistable branch), the transmitted intensity is low as the excitation is out of resonance. However, above a given threshold, polariton-polariton interactions give rise to the energy renormalization of the system, and the σ^+-LPB enters in resonance with the excitation laser, resulting in a high transmission (on state). An analogous curve would be obtained for σ^- polarized excitation.

The data displayed in Fig. 1(a) correspond to the transmission in the center of the spot under purely σ^+ polarized excitation. Let us now consider a spot with a Gaussian spatial profile and elliptically polarized excitation. We can divide the excitation spot into two circularly polarized components: σ^-, in a larger proportion, and σ^+, as depicted in Fig. 1(b). We observe that the D_1 threshold density between the off and on states is not reached in the whole spot at the same time: D_1 is reached at a radius r^- for the σ^- profile, which is bigger than the radius r^+ for the σ^+ profile at the same density. Within these radii the transmission in each polarization is in the on state, with a large density, while outside it is very low (off state). This is what is observed in Fig. 1(c) for an ellipticity of excitation θ (phase shift between the x and y linearly polarized components of the incident light) equal to -0.2π rad (70% σ^-, 30% σ^+), and two different excitation powers. This effect, which arises from the Gaussian distribution of our excitation spot and from the sharp transition from the off to the on state for each polarization, leads to the appearance of a ring in the spatial profile of the transmitted beam with a degree of circular polarization ρ_c close to -1 [$\rho_c = (I^+ - I^-)/(I^+ + I^-)$, $I^{+(-)}$ being the σ^+ (σ^-) transmitted intensity], as shown in the insets of Fig. 1(c). The spin ring, whose size is delimited by r^+ and r^-, is a domain in which the majority of polaritons have the same spin, corresponding to σ^- polarization of emission.

The radius and thickness of the spin ring can be modified by changing, respectively, the total power or the ellipticity of the excitation beam. In the first case, once the center of the spot overcomes the threshold density D_1 with the minority polarization, a spin ring is formed. As the power is increased, both r^+ and r^- increase in size, but the thickness of the ring (r^+ and r^-) does not change noticeably, as evidenced in the insets of Fig. 1(c).

Fine control on the thickness of the spin rings can be obtained by changing the ellipticity of the excitation beam, as the ratio between the σ^+ and σ^- excitation components changes. When the polarization of excitation is close to linear (θ close to 0), the ratio between the σ^+ and σ^- components is almost 1, resulting in similar radii and, consequently, very narrow rings. On the contrary, when the ellipticity of excitation approaches $\pm\pi/2$, the excitation beam is almost purely circularly polarized, leading to a big difference between the radii of both circularly polarized components: the spin rings are wide. This is what is observed in Fig. 2(a), which shows the thickness of the spin rings obtained as a function of the ellipticity of the excitation beam for a power of 77.4 mW. Real-space images of ρ_c corresponding to selected ellipticities are also shown in Fig. 2(a), panels I–VI. In the middle of the spot, ρ_c is almost zero, and it reaches very high values in the ring region. In the external part of the spot, where the transmitted intensity is very low, additional rings are observed. When the ellipticity approaches *zero* we observe a shrinkage of ring thickness, with a minimum value of 3 μm, more than 1 order of magnitude smaller than the spot size.

The fact that the minimum ring size is not obtained for strictly linearly polarized excitation, and the asymmetry observed in Fig. 2 around $\theta = 0$, arise from the presence of an intrinsic weak polarization splitting in our sample, which slightly rotates the pseudospin of injected polaritons [17]. Simulations based on the spin-dependent GPE accounting for this intrinsic splitting [14] quantitatively reproduce our observations, as Fig. 2(b) shows.

In order to understand the results presented in Figs. 1 and 2, we have assumed that α_2 is negligibly small, consistent with previous observations [10,18]. However, the

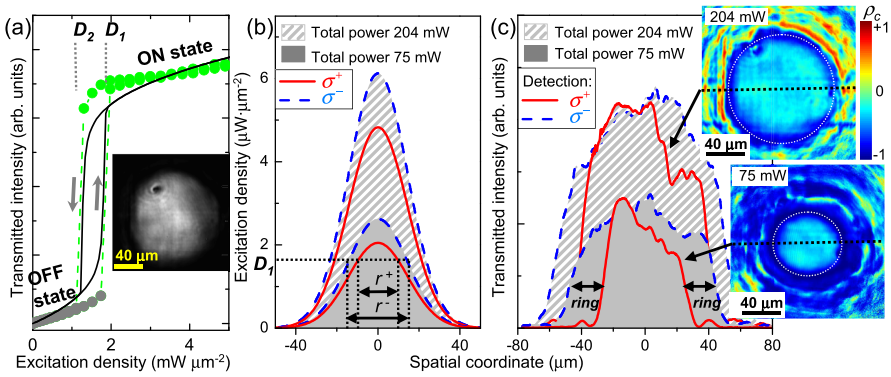

FIG. 1 (color online). (a) Measured (dots) and computed (solid lines) transmission dependence at the center of the spot as a function of excitation density for a purely σ^+ beam. Inset: real-space image in the on state. (b) Computed cross sections passing through the center of a Gaussian spot for the σ^+ and σ^- components of an elliptically polarized beam ($\theta = -0.2\pi$ rad) at two different powers. (c) Experimental profiles of the transmitted intensity resulting in spin rings, as evidenced in the spatially resolved degree of polarization shown in the inset (rings are signaled in white traces). Dashed lines: coordinate from where the profiles in (c) were obtained.

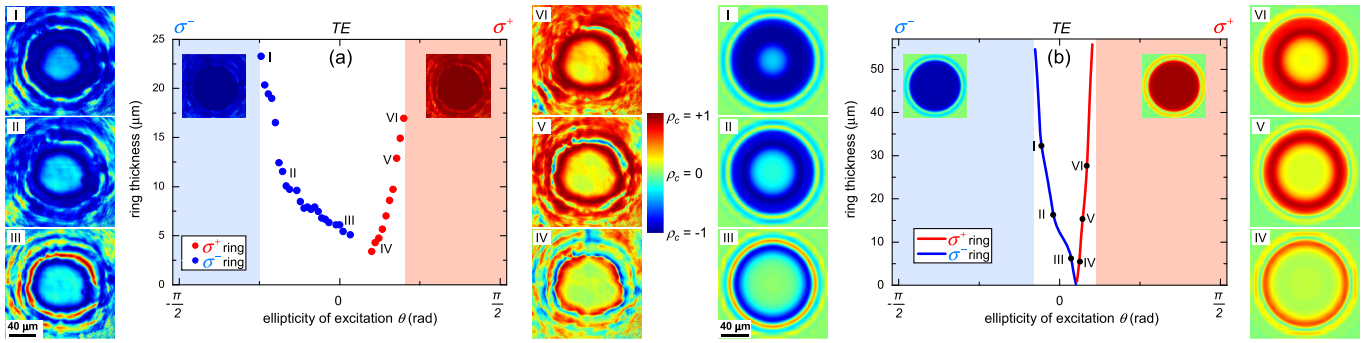

FIG. 2 (color online). Thickness of the spin ring vs ellipticity of the excitation beam (θ) as obtained (a) experimentally and (b) from the simulations. The colored regions indicate the ellipticities for which the whole spot is purely σ^+ or σ^- (see inset). Surrounding images show the transmitted degree of circular polarization, spatially resolved, for selected values of θ.

actual value of α_2 plays an important role when a high density of both $s_z = +1$ and $s_z = -1$ polaritons is simultaneously present in a given region of the sample. This is evidenced in Fig. 3(a), where the transmitted intensity in a small region of 13×13 μm in the center of the spot, resolved into its σ^+ and σ^- components, has been traced with respect to the ellipticity θ of the excitation beam in the conditions of Fig. 2. Let us now analyze in detail the σ^- curve [blue in Fig. 3(a)]. Here the argument will be equivalent for the σ^+ curve. When θ is close to $-\pi/2$, the excitation is purely σ^-. As the excitation density is significantly bigger than D_1, spin-down polaritons lie on the on state, the $s_z = -1$ polariton energy is renormalized to be in resonance with the excitation laser, and the transmitted intensity for the σ^- polarization is high. On the contrary, spin-up polaritons are in the off state. When the ellipticity of excitation is increased to

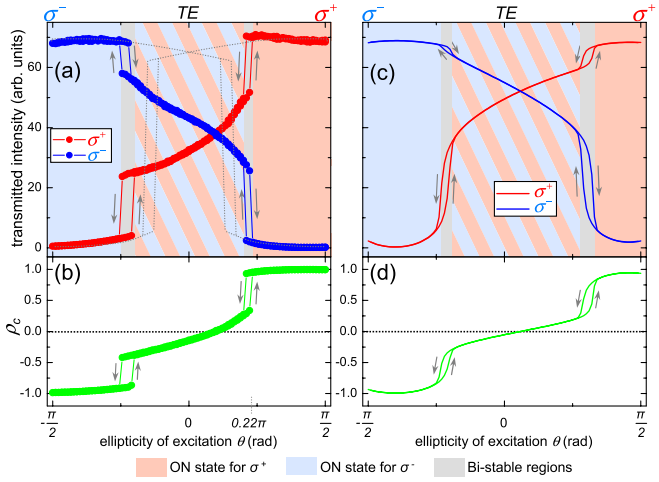

FIG. 3 (color online). Polarization resolved (a) experimental and (c) theoretical dependence of the transmitted intensity with the ellipticity θ of the incident beam, at high excitation power. The arrows mean forward and backward when changing θ. The dotted lines represent the expected behavior if $\alpha_2 = 0$. The degree of circular polarization corresponding to (a) and (c) is depicted in (b) and (d), respectively.

$\theta = -0.21\pi$ rad, the amount of spin-up polaritons is big enough to induce a renormalization of the $s_z = +1$ branch such that the σ^+ component also jumps to the on state. However, they do it to a value of transmitted intensity which is lower than that of the σ^- polaritons at $\theta = -\pi/2$, and simultaneously, the σ^- transmission decreases significantly. This is a direct consequence of the effective interaction between polaritons of the opposite spins, as also reported in [5]. At $k = 0$, the energy of the $s_z = \pm 1$ polaritons is given by

$$E_\pm = E_{\mathrm{LP}}(k = 0) + \alpha_1 |\Psi_\pm|^2 + \alpha_2 |\Psi_\mp|^2 - \frac{i\hbar}{2\tau}, \quad (1)$$

where E_{LP} is the energy of the LPB in the absence of optical excitation, $|\Psi_\pm|^2$ is the $s_z = \pm 1$ polariton density, and τ the polariton lifetime. Indeed, due to the nonzero value of α_2, the presence of a large population of spin-up polaritons for $\theta = -0.21\pi$ rad leads to the change in energy of the spin-down polaritons given by Eq. (1), forcing them out of resonance with the excitation beam, and inducing the decrease of the σ^- transmitted intensity. For the same reason, spin-up polaritons do not reach the high transmitted intensity value expected if $\alpha_2 = 0$, which is sketched in dashed lines in Fig. 3(a). At a value of $\theta = 0.22\pi$ rad, spin-down polaritons fall to the off state, resulting in an increase of the transmitted intensity of the σ^+ polarization, as now the spin-up polariton energy reaches the resonance. When changing the ellipticity in the backward direction, we observe the same phenomena, with slightly different thresholds for the jumps to the on or off state ($\theta = -0.25\pi$ and 0.2π rad), due to the hysteretic behavior of our system.

Figure 3(b) shows the degree of circular polarization corresponding to Fig. 3(a) [see Figs. 3(c) and 3(d) for the corresponding simulations], where we observe that even with a nonzero value of α_2, our system works as a very efficient polarization rectifier, with three possible output states: σ^-, linearly, and σ^+ polarized.

In Figs. 3(a) and 3(b) we have evidenced the effects of a nonzero value of α_2. In Fig. 4 we show an experiment that allows us to calculate its absolute value and sign. In this case

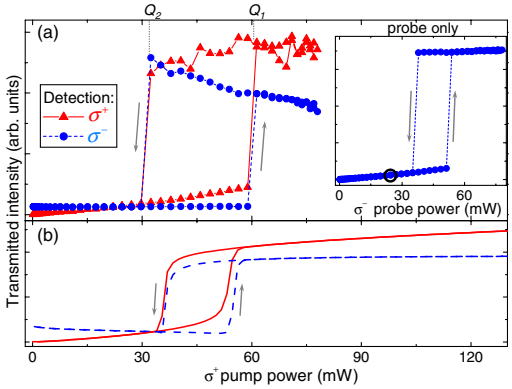

FIG. 4 (color online). (a) Experimental and (b) simulated polarization resolved transmission for a σ^+ pump whose power is varied in the presence of a σ^- probe of fixed power (indicated by a circle in the inset, which shows a power dependence of the probe alone).

we have a σ^- probe beam, blue detuned by 0.2 meV from $E_{\mathrm{LPB}}(k = 0)$, whose power dependence is shown in the inset of Fig. 4(a). We set the power of this probe to the value indicated by the circle, below the lowest point of the hysteresis region. Therefore, the probe beam alone would keep the system in the off state. Now we add a σ^+ pump beam, spatially overlapping the probe, whose density is varied. This is what is shown in Fig. 4(a). The high density of σ^+ pump polaritons at point Q_1 (on state) induces the renormalization of the σ^- polariton energy [as given by Eq. (1)], rendering σ^- polaritons to the on state. This is a clear indication that the sign of the effective α_2 in our conditions is positive (repulsive interaction). A fitting of Eq. (1) to the data shown in Fig. 4(a) is depicted in Fig. 4(b). By performing similar fittings to analogous experiments for different probe powers, we obtain an effective $\alpha_2 = +0.15\alpha_1$, which is the value employed in the simulations based on the spin-dependent GPE presented in Figs. 2(b), 3(c), and 3(d). This result seems to be at odds with recent theoretical [4,7–9,19] and experimental works performed in the optical parametric scattering regime [10,19–21], but in reality it is not, as the effective α_2 may be influenced by a large fraction of dark incoherent excitons which contribute equally to the energy shift in σ^+ and σ^- polarizations [22]. Under coherent excitation, the presence of incoherent excitons can introduce an additional damping mechanism [22]. This effect, which we have neglected in our model, can cause a reduction of the transmitted intensity at high pump powers as observed experimentally [Fig. 4(a)], but does not prevent spin switching and the observation of spin rings. See [14] for further considerations. Our results are in agreement with recent reports under normal incidence pumping in similar microcavities [5,22]. Further experiments are needed to measure the concentration of incoherent quasiparticles in our system.

In this work we have demonstrated the optical creation of spin ring domains in bistable semiconductor microcavities, whose size can be controlled down to the micrometer scale, well below the spot size. This arises from the strongly spin-dependent polariton-polariton interactions, an exceptional property of microcavity polaritons coming from their spin structure and strong light-matter coupling. Our results bring the polariton system closer to the implementation of integrated spin transistors [23] and logic circuits [24,25] with very low thresholds and high potential operation speeds [26].

We thank M. M. Glazov, D. Krizhanovskii, T. Ostatnický, and M. Vladimirova, for fruitful discussions. This work was supported by the ANR (GEMINI 07NANO 07043) and IFRAF. T. L. was supported by NCCR Quantum Photonics. A. B. is a member of the IUF.

[1] M. Kitano, T. Yabuzaki, and T. Ogawa, Phys. Rev. Lett. **46**, 926 (1981); S. Cecchi *et al.*, *ibid.* **49**, 1928 (1982).
[2] J. Stenger *et al.*, Nature (London) **396**, 345 (1998).
[3] I. Zutic, J. Fabian, and S. Das Sarma, Rev. Mod. Phys. **76**, 323 (2004).
[4] N. A. Gippius *et al.*, Phys. Rev. Lett. **98**, 236401 (2007).
[5] T. K. Paraïso *et al.*, Nature Mater. **9**, 655 (2010).
[6] C. Weisbuch *et al.*, Phys. Rev. Lett. **69**, 3314 (1992).
[7] M. Wouters, Phys. Rev. B **76**, 045319 (2007).
[8] M. M. Glazov *et al.*, Phys. Rev. B **80**, 155306 (2009).
[9] T. Ostatnicky, D. Read, and A. V. Kavokin, Phys. Rev. B **80**, 115328 (2009).
[10] P. Renucci *et al.*, Phys. Rev. B **72**, 075317 (2005).
[11] A. Baas *et al.*, Phys. Rev. A **69**, 023809 (2004).
[12] I. A. Shelykh, T. C. H. Liew, and A. V. Kavokin, Phys. Rev. Lett. **100**, 116401 (2008).
[13] I. A. Shelykh *et al.*, Phys. Rev. Lett. **97**, 066402 (2006).
[14] See supplementary material at http://link.aps.org/supplemental/10.1103/PhysRevLett.105.216403 for the parameters employed in the spin-dependent Gross-Pitaevskii model, and a discussion on the evaluation of α_2.
[15] R. Houdré *et al.*, Phys. Rev. B **61**, R13333 (2000).
[16] A. Amo *et al.*, Nature Phys. **5**, 805 (2009).
[17] A. Amo *et al.*, Phys. Rev. B **80**, 165325 (2009).
[18] D. Ballarini *et al.*, Appl. Phys. Lett. **90**, 201905 (2007).
[19] M. Vladimirova *et al.*, Phys. Rev. B **82**, 075301 (2010).
[20] D. N. Krizhanovskii *et al.*, Phys. Rev. B **73**, 073303 (2006).
[21] C. Leyder *et al.*, Phys. Rev. Lett. **99**, 196402 (2007).
[22] D. Sarkar *et al.*, preceding Letter, Phys. Rev. Lett. **105**, 216402 (2010).
[23] R. Johne *et al.*, Phys. Rev. B **81**, 125327 (2010).
[24] T. C. H. Liew, A. V. Kavokin, and I. A. Shelykh, Phys. Rev. Lett. **101**, 016402 (2008).
[25] T. C. H. Liew *et al.*, Phys. Rev. B **82**, 033302 (2010).
[26] A. Amo *et al.*, Nat. Photon. **4**, 361 (2010).